

## Nearest-neighbor functions in a one-dimensional generalized ballistic deposition model

P. Viot,<sup>1</sup> P. R. Van Tassel,<sup>2</sup> and J. Talbot<sup>3</sup>

<sup>1</sup>Laboratoire de Physique Théorique des Liquides, Université Pierre et Marie Curie, 4, place Jussieu 75252 Paris Cedex 05, France

<sup>2</sup>Department of Chemical Engineering and Materials Science, Wayne State University,  
5050 Anthony Wayne Drive, Detroit, Michigan 48202

<sup>3</sup>Department of Chemistry and Biochemistry, Duquesne University, Pittsburgh, Pennsylvania 15282

(Received 7 November 1996; revised manuscript received 16 June 1997)

We derive exact expressions for the nearest-neighbor probability functions for configurations of disks on a line generated by a generalized ballistic deposition process. The presence of clusters of disks profoundly modifies the nearest-neighbor functions compared with those of cluster-free configurations. We generalize theorems on ergodic ensembles of isotropic packing of particles to cases where clustering of particles occurs. [S1063-651X(98)02602-6]

PACS number(s): 61.20.-p, 05.20.-y

### I. INTRODUCTION

Nearest-neighbor distribution functions of many-particle systems, which provide the probability of finding a nearest neighbor at a given distance from some reference point, are indispensable in the study of the liquid state and amorphous solids [1–7], transport processes in heterogeneous materials [8,9], and spatial patterns in biological systems [10].

In a pioneering work, Hertz [11] obtained exact expressions for the nearest-neighbor functions for a system of randomly distributed point particles in a three-dimensional space. More recently, Torquato, Lu, and Rubinstein [4], showed how to express these functions in terms of the infinite set of  $n$ -particle density functions  $\rho_1, \rho_2, \dots, \rho_n$  ( $n \rightarrow \infty$ ). For the random point model, which has a trivial structure, it is possible to recover Hertz's result by summing the series exactly. Interacting particle systems are much more challenging since one does not in general have a complete knowledge of the  $\{\rho_n\}$ . An important exception is the class of one-dimensional systems, which are usually amenable to exact analysis. We note also that accurate approximate expressions have been developed for equilibrium systems of hard disks ( $D=2$ ) and hard spheres ( $D=3$ ) [3].

Using the notation of Ref. [12], the nearest-neighbor functions for the void quantities are defined as follows: (i)  $H_V dr$  is the probability that at an *arbitrary point* in the system the center of the nearest particle lies at a distance between  $r$  and  $r + dr$ , (ii)  $E_V$  is the probability of finding a circular cavity of radius  $r$  centered at some *arbitrary point*, empty of disk centers. (iii)  $2\rho G_V dr$  is the probability that, given a region of length  $2r$  centered at an *arbitrary point* in the system that is empty of rod centers, rod centers are contained in the shell of thickness  $2dr$  enclosing the region. The particle quantities,  $H_P$ ,  $E_P$ ,  $G_P$ , are similar except "rod center" replaces "arbitrary point" in the above definitions.

It follows from the definitions given above that  $E_V$  is related to  $H_V$  by the relation

$$H_V = - \frac{\partial E_V}{\partial r} \quad (1)$$

and  $G_V$  to  $H_V$  by

$$G_V = \frac{H_V}{2\rho E_V(r,t)}. \quad (2)$$

Thus, from the knowledge of either  $H_V$  or  $E_V$  one can derive exact expressions for the remaining two functions using Eqs. (1) and (2). Identical equations can be established for particle quantities  $H_P$  and  $G_P$ .

Although equilibrium configurations of particles represent an obvious class of model system, it is also of interest to examine the nearest-neighbor functions of nonequilibrium configurations such as those generated by the random sequential adsorption (RSA) process. These systems are also of interest in relation to some general theorems concerning the mean nearest-neighbor distance, which may be readily calculated from the nearest-neighbor functions, in random packings of hard particles. These theorems, recently proved by Torquato [7], suggest that the nearest-neighbor functions for particles deposited by the RSA mechanism are quite different from their equilibrium counterparts. This was confirmed in the recent work of Rintoul *et al.* [12] who obtained exact expressions for the nearest-neighbor functions for configurations of rods deposited on a line by the RSA process.

The present paper is motivated in part by the observation that the theorems of Torquato do not consider the possibility of clustering. We first derive the nearest-neighbor functions for configurations of disks deposited on a line by generalized ballistic deposition (GBD), an irreversible space filling process that leads to the formation of connected particle clusters of different sizes. In one dimension, the kinetics and the distribution of cluster sizes have been obtained exactly [13]. In two dimensions, the model provides a quantitative description of adsorbed configurations of colloidal particles on solid surfaces [14]. The basic quantities for the GBD model are defined and derived in Sec. II. The void and particle functions are then obtained (Sec. III), as well as an exact expression for the mean nearest-neighbor distance. It is worth noting that we recover here the results of Rintoul *et al.* [12] with an approach that is somewhat simpler than that

employed by these authors. Extended theorems for isotropic packings are given in Sec. IV.

## II. GENERALIZED BALLISTIC DEPOSITION MODEL

In one dimension, the GBD model is defined as follows: hard disks of diameter  $\sigma$  (set equal to unity) are deposited onto an infinite line sequentially, uniformly, and at a constant rate per unit length. If a trial particle does not encounter any preadsorbed disk, it adsorbs with a probability  $p$ . Otherwise, it is rejected. If the trial particle is above a preadsorbed disk, it rolls towards the surface up to one preadsorbed disk by following the path of steepest descent; if it eventually reaches the line, the new disk is accepted with a probability  $p'$  and if not, it is rejected. Using appropriate dimensionless variables, one can see that the process depends only on the ratio  $a=p'/p$ : for  $a=0$ , only direct adsorption is allowed, which corresponds to the random sequential adsorption (RSA) process [13]. For  $a=1$ , we recover the ballistic deposition model [15]. In the limit  $a \rightarrow +\infty$ , only deposition following contact with a preadsorbed disk is permitted after a first seed particle is inserted, and this results in a close-packed configuration. The parameter  $a$  is thus a measure of the efficiency of cluster formation.

If  $\rho(t)$  denotes the number density of particles on the line at dimensionless time  $t$ , the kinetics of the GBD model is given by the following rate equation:

$$\frac{d\rho(t)}{dt} = P(l=1,t) + 2aP_1(l=1,t), \quad (3)$$

where  $P(l,t)$  is the probability density of finding a cavity (i.e., an empty interval) of diameter *at least*  $l$  and  $P_1(l,t)$  is the probability of finding a cavity of length *at least*  $l$  bounded on at least one side by a particle.  $P(l,t)$  is then simply the cumulative probability function of  $P_1(l,t)$ ,

$$P(l,t) = \int_l^{+\infty} du P_1(u,t). \quad (4)$$

To determine  $P(l,t)$ , we note that a cavity of diameter  $l \geq 1$  can be destroyed by inserting particles that can either lie completely within this cavity or can partially overlap the right or the left sides of the cavity [16]. The time evolution of the probability function  $P(l,t)$  can then be expressed as

$$-\frac{\partial P(l,t)}{\partial t} = (l-1)P(l,t) + 2 \int_0^1 du P(l+u,t) + 2a \int_0^1 du P_1(l+u,t) \quad \text{for } l \geq 1. \quad (5)$$

Inserting the ansatz

$$P(l,t) = h_a^2(t) \exp[-(l-1)t] \quad (6)$$

in Eqs. (4) and (5) with the initial condition  $P(l,t=0) = 1$  gives

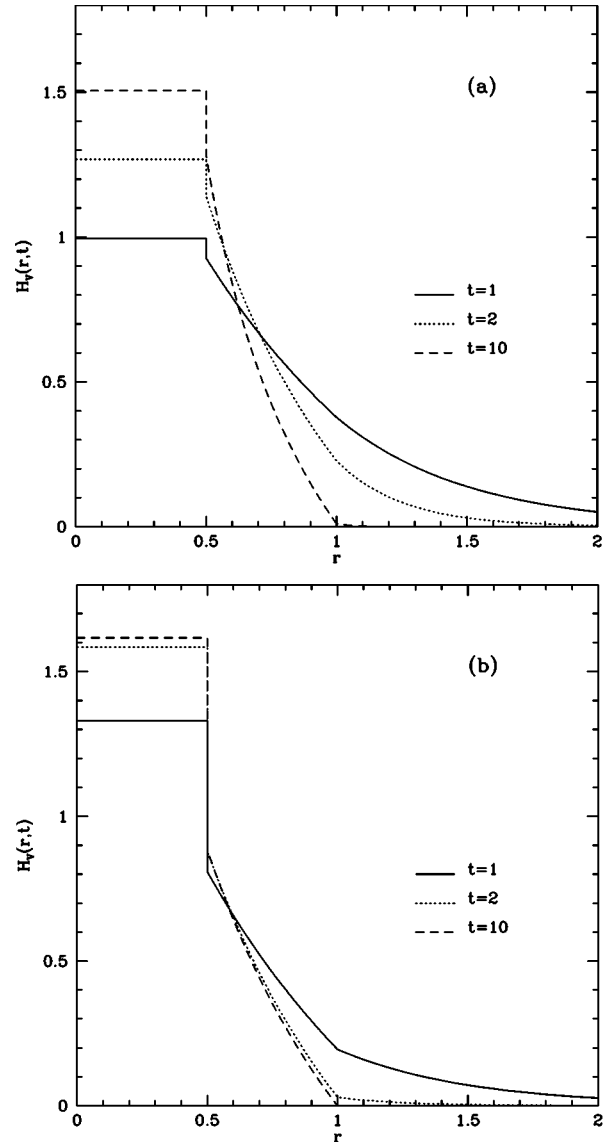


FIG. 1.  $H_v(r,t)$  vs the distance  $r$  at different times ( $t = 1, 2, 10$ ) and for two values of  $a$ : (a)  $a=0.1$ , (b)  $a=1$ .

$$h_a(t) = \exp\left(-\int_0^t \frac{1-e^{-u}}{u} du + a(1-t-e^{-t})\right), \quad (7)$$

and the number density of particles is then equal to

$$\rho(t) = \int_0^t dt_1 (1 + 2at_1) h_a^2(t_1). \quad (8)$$

Notice that the saturation state is reached exponentially,  $\rho(\infty) - \rho(t) \sim \exp(-2at)/(at)$ , for all nonzero values of  $a$ , whereas for  $a=0$  (corresponding to the car parking problem [17]), the asymptotic kinetics is algebraic,  $\rho(\infty) - \rho(t) \sim 1/t$ .

## III. NEAREST-NEIGHBOR FUNCTIONS

### A. Void quantities

For  $r \leq 1/2$ , because multiple overlaps are prohibited,  $H_v(r,t)$  is just twice the particle density,

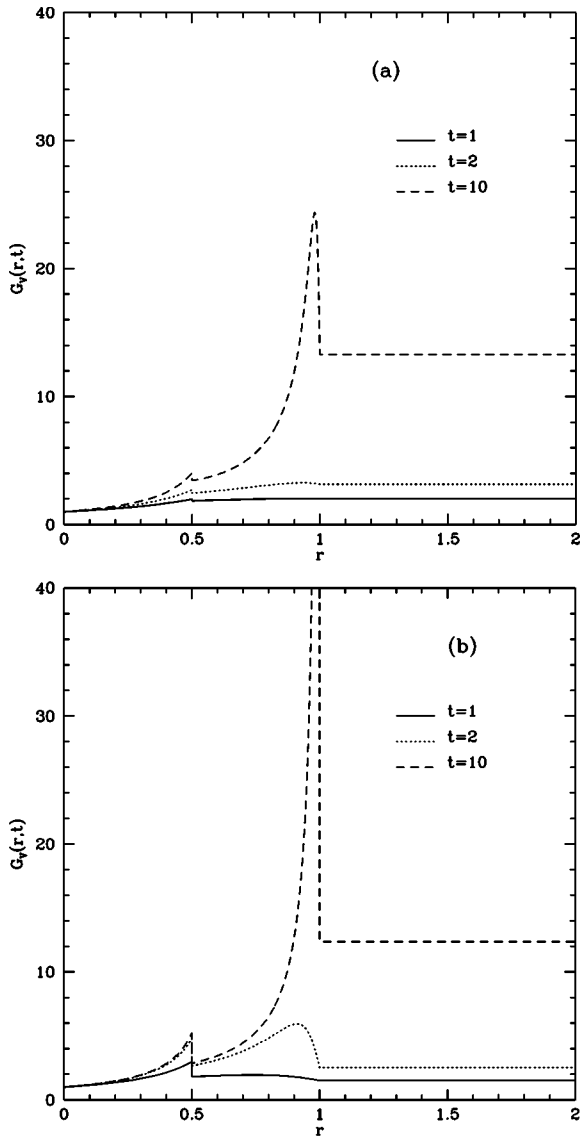


FIG. 2.  $G_V(r,t)$  vs the distance  $r$  at different times ( $t = 1, 2, 10$ ) and for two values of  $a$ : (a)  $a = 0.1$ , (b)  $a = 1$ .

$$H_V(r,t) = 2\rho(t), \quad r \leq 1/2. \tag{9}$$

Combining Eqs. (1) and (2), one deduces that

$$E_V(r,t) = 1 - 2r\rho(t), \quad r \leq 1/2, \tag{10}$$

$$G_V(r,t) = \frac{1}{1 - 2r\rho(t)}, \quad r \leq 1/2. \tag{11}$$

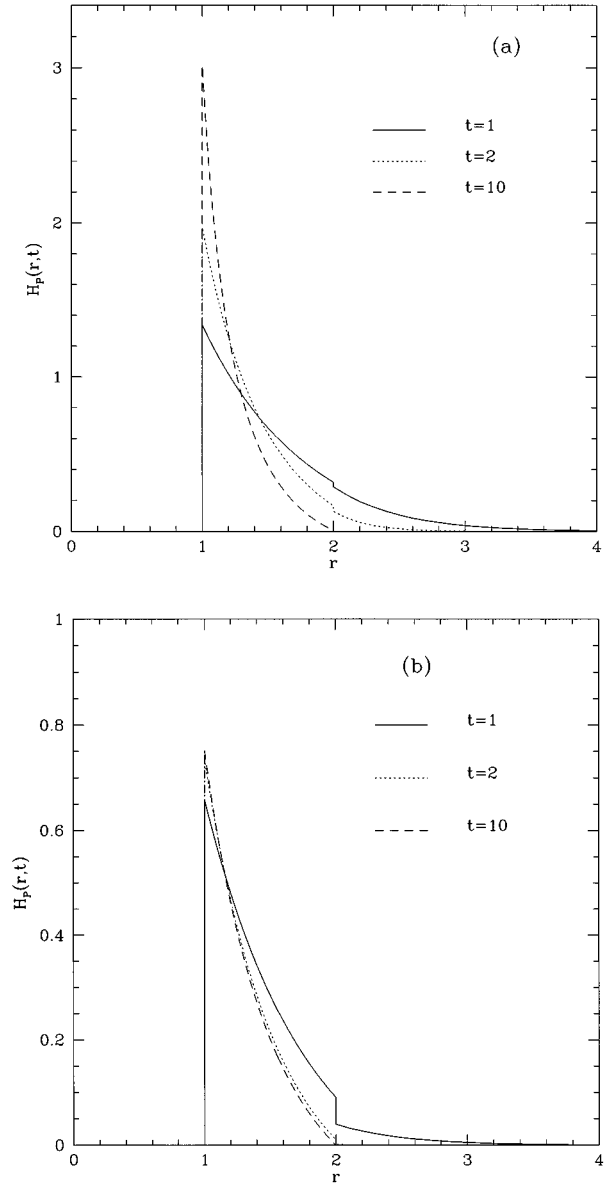


FIG. 3.  $H_P(r,t)$  vs the distance  $r$  at different times ( $t = 1, 2, 10$ ) and for two values of  $a$ : (a)  $a = 0.1$ , (b)  $a = 1$ .

When  $r \geq 1/2$ , since  $E_V(r,t)$  is the probability of finding a void of radius  $r$  (or diameter  $2r$ ) empty of rod centers, one has  $E_V(r,t) = P(2r - 1, t)$  and  $H_V(r,t) = 2P_1(2r - 1, t)$ .

For  $1/2 \leq r \leq 1$ , one has  $0 \leq 2r - 1 \leq 1$ . Therefore,  $E_V(r,t)$  and  $H_V(r,t)$  are given by the knowledge of  $P_1(l,t)$  for  $0 \leq l \leq 1$ . Considering all ways of creation and destruction of a cavity of length at least  $l$  bounded on a side by a particle, the time evolution of the probability function  $P_1(l,t)$  can be expressed as

$$\frac{\partial P_1(l,t)}{\partial t} = - \int_{\text{Max}(0,1-l)}^1 du P_1(l+u,t) + P(1+l,t) - a \left( \int_{\text{Max}(0,1-l)}^1 du P_2(l+u,t) + P_1(1,t) - P_1(1+l,t) \right) \quad \text{for } l < 1, \tag{12}$$

where  $P_1(l,t)$  is the cumulative probability function of  $P_2(l,t)$ . Notice that for  $0 < l < 1$ ,  $P_1(l,t)$  depends on probability functions for values of  $l > 1$  that can be derived from Eq. (6). Following a calculation, one obtains

$$P_1(l,t) = 2 \int_0^t dt' h_a^2(t') e^{-lt'} (1 + at') - \rho(t), \quad (13)$$

which gives

$$H_V(r,t) = 2 \left( \int_0^t dt' 2h_a^2(t') e^{-(2r-1)t'} (1 + at') - \rho(t) \right), \quad (14)$$

$$E_V(r,t) = 1 - 2(1-r)\rho(t) - 2 \int_0^t dt' h_a^2(t') \times (1 + at') \frac{1 - e^{-(2r-1)t'}}{t'}, \quad (15)$$

with  $G_V(r,t)$  determined from  $E_V(r,t)$  and  $H_V(r,t)$ .

If  $r \geq 1$ , the void quantities are simply obtained from Eq. (6):

$$E_V(r,t) = h_a^2(t) \exp[-2(r-1)t], \quad (16)$$

and, therefore,

$$H_V(r,t) = 2th_a^2(t) \exp[-2(r-1)t], \quad (17)$$

$$G_V(r,t) = \frac{t}{\rho(t)}. \quad (18)$$

Figure 1 displays  $H_V(r,t)$  for  $a=0.1$  and  $a=1.0$  and  $t=1,2,10$ . Note the finite discontinuity at  $r=0.5$  and the cusp at  $r=1$ , which increase when  $a$  or  $t$  gets bigger.

The function  $G_V(r,t)$  is shown in Fig. 2. It has the expected discontinuity at  $r=0.5$ , consistent with the behavior of  $H_V(r,t)$ . In addition, a striking peak emerges in the neighborhood of  $r=1$  when  $t$  is larger than  $1/a$ . As we have previously noted this function is, contrary to appearances at long times, *continuous* at  $r=1$  and its apparent divergence can be understood by examining the behavior of  $H_V(r,t)$  and  $E_V(r,t)$  for  $r$  close to 1: From Eq. (14), the Taylor series for  $H_V(r,t)$  at  $r=1$  gives  $H_V(r,t) = a_1 + b(1-r)$  where  $a_1 > 0$  and  $b > 0$  and  $a_1 \ll b$ , if  $t > 1/a$ . Similarly, one obtains for  $E_V(r,t)$ ,  $E_V(r,t) = a_2 + a_1(1-r) + b/2(1-r)^2$  where  $a_2 > 0$  and  $a_2 \approx a_1$ . A simple analysis of the ratio  $H_V(r,t)/E_V(r,t)$  shows that, although the function  $G_V(r,t)$  seems to diverge when  $r$  is close to 1, it instead reaches a maximum value for  $r_c = 1 - \sqrt{a_2/b}$  and then decreases very rapidly between  $r_c$  and 1. Clearly, the presence of clusters on the line significantly modifies the structure (of the void probability functions) compared with the RSA model [12]. Spectacular differences have already been noted in the pair correlations of the GBD model [16].

## B. Particle quantities

Because of the hard-core interaction that prevents particle overlap, the particle nearest-neighbor functions have simple expressions for  $0 \leq r \leq 1$ :

$$E_P(r,t) = 1, \quad H_P(r,t) = 0, \quad G_P(r,t) = 0. \quad (19)$$

At  $r=1$ ,  $H_P(r,t)$  has a  $\delta$ -singularity due to the existence of particles at contact [13]. Denoting the singular part of  $H_P(r,t)$  at  $r=1$  as  $H_P(r,t) = \delta(r-1)h_P(t)$ , one finds

$$h_P(t) = \frac{4a}{\rho(t)} \int_0^t dt_1 t_1 h_a^2(t_1) - \frac{2a^2}{\rho(t)} \int_0^t dt_1 h_a(t_1) e^{-at_1} \int_0^{t_1} dt_2 h_a(t_2) e^{at_2} \left( \frac{e^{-2at_2} - e^{-2t_2}}{2(1-a)} + t_2 e^{-t_2} \right). \quad (20)$$

Consequently,  $E_P(r,t)$ , which is the cumulative probability of  $H_P(r,t)$ , exhibits a discontinuity at  $r=1$ .

When  $r \geq 1$ , since  $E_P(r,t)$  is the probability of finding a void of a radius  $r$  (or diameter  $2r$ ) empty of rod centers centered on a rod center, one has

$$\rho E_P(r,t) = P(r-1, r-1, t), \quad (21)$$

$$\rho H_P(r,t) = 2P_1(r-1, r-1, t), \quad (22)$$

where  $P(r-1, r-1, t)$  denotes respectively the probability of finding two neighboring cavities of diameter *at least*  $r-1$  separated by one particle, and  $P_1(r-1, r-1, t)$  the probability density of finding two neighboring cavities, one of diameter  $r-1$  and another of diameter *at least*  $l_2$  separated by one particle. Exact expressions of the cavity functions,  $P(r-1, r-1, t)$  and  $P_1(r-1, r-1, t)$ , can be obtained. Details of the calculation are given in the Appendix.

For  $1 \leq r \leq 2$ , inserting Eqs. (A6) and (A7) in Eqs. (21) and (22) leads to

$$\begin{aligned} \rho(t) E_P(r,t) &= \int_0^t dt_1 h_a^2(t_1) \left\{ e^{-2(r-1)t_1} - 2 \left[ (1 + at_1) \left( \frac{1 - e^{-(r-1)t_1}}{t_1} \right) + a \right] \frac{e^{-2at_1} - e^{-2t_1}}{2(1-a)} \right\} \\ &+ 2 \int_0^t dt_1 h_a(t_1) e^{-at_1} \left( (1 + at_1) \frac{1 - e^{-(r-1)t_1}}{t_1} + a \right) \int_0^{t_1} dt_2 h_a(t_2) e^{at_2} (e^{-t_2} - e^{-(r-1)t_2}) \\ &\times \left[ (1 + at_2) \frac{e^{-2at_2} - e^{-2t_2}}{2(1-a)t_2} + e^{-t_2} \right], \end{aligned} \quad (23)$$

and

$$\begin{aligned}
\rho(t)H_p(r,t) &= \int_0^t dt_1 h_a^2(t_1) \left[ 2t_1 e^{-2(r-1)t_1} - 2(1+at_1)e^{-(r-1)t_1} \frac{e^{-2at_1} - e^{-2t_1}}{2(1-a)} \right] \\
&\quad - 2 \int_0^t dt_1 h_a(t_1) e^{-at_1} (1+at_1) e^{-(r-1)t_1} \int_0^{t_1} dt_2 h_a(t_2) e^{at_2} (e^{-t_2} - e^{-(r-1)t_2}) \left[ (1+at_2) \frac{e^{-2at_2} - e^{-2t_2}}{2(1-a)t_2} + e^{-t_2} \right] \\
&\quad - 2 \int_0^t dt_1 h_a(t_1) e^{-at_1} \left( (1+at_1) \frac{1 - e^{-(r-1)t_1}}{t_1} + a \right) \int_0^{t_1} dt_2 h_a(t_2) e^{at_2} e^{-(r-1)t_2} \\
&\quad \times \left[ (1+at_2) \frac{e^{-2at_2} - e^{-2t_2}}{2(1-a)} + t_2 e^{-t_2} \right]. \tag{24}
\end{aligned}$$

Using Eqs. (19) and (23) one can verify that  $E_p(r=1-) - E_p(r=1+) = h_p$ .

For  $r \geq 2$ , combining Eqs. (21) and (22) and Eq. (A4) yields

$$E_p(r,t) = \frac{h_a^2(t)}{\rho(t)} \frac{e^{-2at} - e^{-2t}}{2(1-a)} e^{-2(r-2)t}, \tag{25}$$

$$H_p(r,t) = \frac{2th_a^2(t)}{\rho(t)} \frac{e^{-2at} - e^{-2t}}{2(1-a)} e^{-2(r-2)t}. \tag{26}$$

So, for  $r \geq 2$ ,  $G_p(r,t)$  and  $G_v(r,t)$  are identical and independent of  $r$ .

It is worth noting that, for  $a > 0$ ,  $H_p(r,t)$  and  $G_p(r,t)$  are discontinuous at  $r=2$ . Figure 3 shows the regular part of  $H_p(r,t)$  for  $a=0.1, 1.0$  and for different times. A strong peak in  $G_p(r,t)$  occurs for  $r$  close to 1 (Fig. 4). An argument similar to that which we have given for  $G_v(r,t)$  explains this striking behavior. Even for a small value of  $a$ , corresponding to a relatively weak clustering effect, the nearest-neighbor functions are strongly modified compared to those obtained by an RSA process [12]. Note that Eq. (24) with  $a=0$  corrects Eq. (48) of Ref. [12] in which a term is missing in the last line of the equation (Fig. 4 of Ref. [12] is, however, correct).

Finally, knowledge of  $E_p(r,t)$  allows us to calculate the mean nearest-neighbor distance  $\lambda$  as

$$\begin{aligned}
\lambda &= 1 + \int_1^\infty dr E_p(r,t) = 1 + \frac{h_a^2(t)}{2t\rho(t)} \frac{e^{-2at} - e^{-2t}}{2(1-a)} + \frac{1}{\rho(t)} \int_0^t dt_1 h_a^2(t_1) \left\{ \frac{1 - e^{-2t_1}}{2t_1} - 2 \frac{e^{-2at_1} - e^{-2t_1}}{2(1-a)} \right. \\
&\quad \times \left[ (1+at_1) \left( \frac{1}{t_1} - \frac{1 - e^{-t_1}}{t_1^2} \right) + a \right] \left. \right\} + \frac{2}{\rho(t)} \int_0^t dt_1 h_a(t_1) e^{-at_1} \int_0^{t_1} dt_2 h_a(t_2) e^{at_2} \left[ (1+at_2) \frac{e^{-2at_2} - e^{-2t_2}}{2(1-a)t_2} + e^{-t_2} \right] \\
&\quad \times \left\{ \left[ (1+at_1) \left( \frac{1}{t_1} - \frac{1 - e^{-t_1}}{t_1^2} \right) + a \right] e^{-t_2} + \left( \frac{1+at_1}{t_1} \right) \frac{1 - e^{-(t_1+t_2)}}{t_1+t_2} - \left( \frac{1+2at_1}{t_1} \right) \frac{1 - e^{-t_2}}{t_2} \right\}. \tag{27}
\end{aligned}$$

At small densities, the mean nearest-neighbor distance becomes

$$\lambda \approx \frac{1}{2\rho} + 1. \tag{28}$$

This has the same leading behavior  $[\rho(t)^{-1}]$  at low density as the equilibrium sticky hard rod system [18] at number density  $\rho$ , for which the exact expression for  $\lambda$  is

$$\lambda = 1 + \exp\left(\frac{-2a\beta P}{1+a\beta P}\right) \frac{1+a\beta P}{2a\beta P}, \tag{29}$$

where  $P$  is related to  $\rho$  by the equation of state [16]:

$$\beta P = \frac{1}{2a} \left[ \sqrt{1 + \frac{4a\rho}{1-\rho}} - 1 \right]. \tag{30}$$

The dependence of  $\lambda$  on  $\rho$ , for several values of the stickiness parameter  $a$ , is illustrated in Fig. 5. The mean distance  $\lambda$  between nearest neighbors for the sticky hard rod system *increases* with  $a$  for a given value of the density of particles, whereas  $\lambda$  decreases with  $a$  for the GBD model. Consequently,  $\lambda$  for the sticky hard rod system, which is smaller than  $\lambda$  for the GBD process when  $a$  is small, becomes larger when  $a$  increases. This amazing feature can be interpreted by the fact that particle configurations are more correlated at equilibrium than in the GBD process where deposited particles cannot move once adsorbed.

#### IV. THEOREMS ON ISOTROPIC PACKINGS

The theorems on isotropic packings of identical  $D$ -dimensional hard spheres derived by Torquato [7] do not consider systems in which clusters can be formed. Clusters occur at equilibrium when interactions between particles

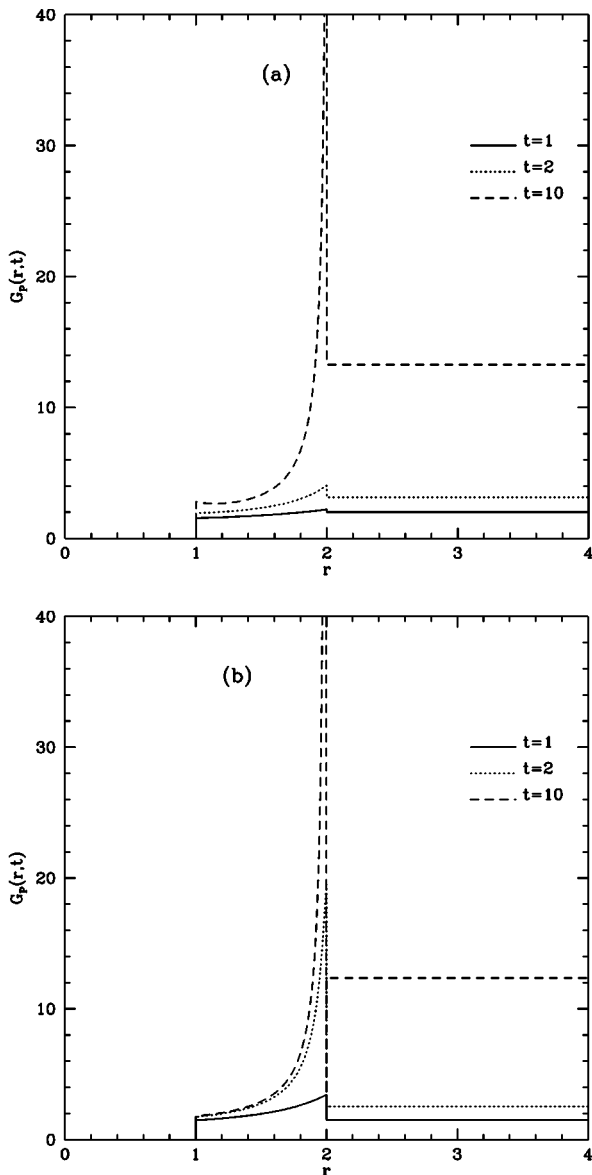


FIG. 4.  $G_p(r,t)$  vs the distance  $r$  at different times ( $t=1,2,10$ ) and for two values of  $a$ : (a)  $a=0.1$ , (b)  $a=1$ .

contain a singular attractive part, as in the sticky hard rod system [18] and in nonequilibrium processes, like the GBD model studied here. Using the definition of  $G_p(r,t)$ , it is easy to convince oneself that for a system of clusters, a  $\delta$ -singularity arises at contact but at larger distances the function  $G_p$  is continuous or exhibits at most finite discontinuities. Therefore, two theorems of Ref. [12] should be rewritten as follows:

*Theorem 1:* For any ergodic ensemble of isotropic packings of identical,  $D$ -dimensional hard spheres in which clustering is allowed and  $G_p(1+) \leq G_p(r)$  for  $1 < r \leq \infty$ ,

$$\lambda \leq 1 + \frac{\exp(-2^D D \phi G_p^s)}{D 2^D \phi G_p(1+)}, \quad (31)$$

where  $G_p(1+)$  denotes the left limit at  $r=1$  of the regular part of  $G_p(r)$ ,  $G_p^s$  the amplitude of the  $\delta$  singularity of  $G_p$  at  $r=1$  and  $\phi$  the packing fraction.

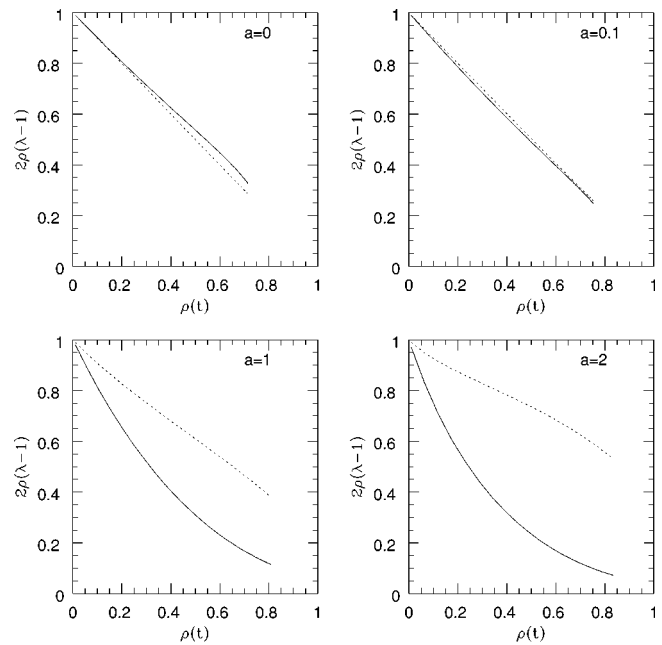


FIG. 5. Mean distance between nearest-neighbor particles vs density for various values of  $a$  ( $a=0,0.1,1,2$ ). The full curves correspond to the GBD model and the dashed curves correspond to the sticky hard rod model.

*Theorem 2:* For any ergodic ensemble of isotropic packings of identical,  $D$ -dimensional hard spheres in which clustering is allowed and  $(1-\phi)^{-1} \leq G_p(r)$  for  $1 < r \leq \infty$ ,

$$\lambda \leq 1 + (1-\rho) \frac{\exp(-2^D D \rho G_p^s)}{D 2^D \rho}. \quad (32)$$

Proofs of these theorems proceed in a fashion very similar to that in Ref. [7] and are not reproduced here. As  $G(r)$  has no simple lower bound for any ergodic hard-sphere system with clustering, one cannot find a corresponding Theorem 3 that gives an upper bound for the mean nearest-neighbor distance [7]. Note that when the singularity in  $G_p$  disappears, as, for instance, when  $a$  goes to 0 in the GBD model, one recovers, as expected, the results obtained by Torquato [7].

### V. SUMMARY

We have derived analytic expressions for the nearest-neighbor distribution functions associated with a one-dimensional configuration of rods generated by a generalized ballistic deposition process. The clustering mechanism that occurs in GBD profoundly modifies the shape of the nearest-neighbor functions. Theorems on ergodic ensembles of isotropic packing of particles have been generalized to include the case when clusters are present and were tested against the results obtained for the generalized ballistic deposition model.

### ACKNOWLEDGMENTS

This work has been supported in part by a CNRS-NSF grant. The Laboratoire de Physique Théorique des Liquides is Unité de Recherche Associée No. 765 au Centre National de la Recherche Scientifique.

## APPENDIX

In order to obtain expressions for the particle nearest-neighbor functions, we introduce three cavity probability functions:  $P(l_1, l_2, t)$  denotes the probability of finding two neighboring cavities, one of diameter *at least*  $l_1$  and another of diameter *at least*  $l_2$  separated by one particle,  $P_1(l_1, l_2, t)$  the probability density of finding two neighboring cavities, one of diameter  $l_1$  and another of diameter *at least*  $l_2$  separated by one particle, and  $P_2(l_1, l_2, t)$  the probability density of finding two neighboring cavities, one of diameter *at least*  $l_1$  and another of diameter  $l_2$  separated by one particle.

$P(l_1, l_2, t)$  is then the cumulative probability density of  $P_1(l_1, l_2, t)$  and  $P_2(l_1, l_2, t)$ :

$$P(l_1, l_2, t) = \int_{l_1}^{+\infty} du P_1(u, l_2, t), \quad (\text{A1})$$

$$P(l_1, l_2, t) = \int_{l_2}^{+\infty} du P_2(l_1, u, t). \quad (\text{A2})$$

A kinetic equation can be written in a closed form:

$$\begin{aligned} \frac{\partial P(l_1, l_2, t)}{\partial t} = & -[\text{Max}(0, l_1 - 1) + \text{Max}(0, l_2 - 1)]P(l_1, l_2, t) - \int_{\text{Max}(0, 1 - l_1)}^1 du P(l_1 + u, l_2, t) - \int_{\text{Max}(0, 1 - l_2)}^1 du P(l_1, l_2 + u, t) \\ & + P(l_1 + l_2 + 1, t) - a \left( P[\text{Max}(1, l_1), l_2, t] + P(l_1, \text{Max}(1, l_2), t) - \int_{\text{Max}(0, 1 - l_1)}^1 du P_1(l_1 + u, l_2, t) \right. \\ & \left. - \int_{\text{Max}(0, 1 - l_2)}^1 du P_2(l_1, l_2 + u, t) \right). \end{aligned} \quad (\text{A3})$$

The strategy to solve these coupled equations consists of considering the case  $l_1 \geq 1$  and  $l_2 \geq 1$ . Using the ansatz  $P(l_1, l_2, t) = F(t)e^{-(l_1 + l_2 - 2)t}$  in Eq. (A3) leads to a time differential equation for  $F(t)$ , which gives after calculation

$$P(l_1, l_2, t) = h_a^2(t) \frac{e^{-2at} - e^{-2t}}{2(1-a)} e^{-(l_1 + l_2 - 2)t}. \quad (\text{A4})$$

For  $0 \leq l_1 < 1$  and  $l_2 \geq 1$  using the ansatz

$$P(l_1, l_2, t) = h_a(t)p(l_1, t)e^{-(l_2 - 1)t}, \quad (\text{A5})$$

and Eq. (A4), Eq. (A3) can be integrated and one obtains

$$p(l_1, t) = h_a(t) \frac{e^{-2at} - e^{-2t}}{2(1-a)} - e^{-at} \int_0^t dt_1 h_a(t_1) e^{at_1} (e^{-t_1} - e^{-l_1 t_1}) \left[ (1 + at_1) \frac{e^{-2at_1} - e^{-2t_1}}{2(1-a)t_1} + e^{-t_1} \right]. \quad (\text{A6})$$

For  $0 \leq l_2 < 1$  and  $l_1 \geq 1$ ,  $P(l_1, l_2, t)$  is obtained from Eq. (A5) by permuting  $l_1$  with  $l_2$ .

Finally, for  $0 \leq l_1 \leq 1$  and  $0 \leq l_2 \leq 1$ , Eq. (A3) can also be integrated and  $P(l_1, l_2, t)$  is expressed as

$$P(l_1, l_2, t) = \int_0^t dt_1 h_a(t_1) \left[ h_a(t_1) e^{-(l_1 + l_2)t_1} - a[p(l_1, t_1) + p(l_2, t_1)] - (1 + at_1) \left( \frac{1 - e^{-l_1 t_1}}{t_1} p(l_2, t_1) + \frac{1 - e^{-l_2 t_1}}{t_1} p(l_1, t_1) \right) \right]. \quad (\text{A7})$$

- 
- [1] J. G. Berryman, Phys. Rev. A **27**, 1053 (1983).  
 [2] H. Reiss and A. D. Hammerich, J. Phys. Chem. **90**, 6252 (1986).  
 [3] S. H. Simon, V. Dobrosavljevic, and R. M. Stratt, J. Chem. Phys. **94**, 7360 (1991).  
 [4] S. Torquato, B. Lu, and J. Rubinstein, Phys. Rev. A **41**, 2059 (1990).  
 [5] U. F. Edgal, J. Chem. Phys. **94**, 8191 (1991).  
 [6] J. R. MacDonald, J. Phys. Chem. **96**, 3861 (1992).  
 [7] S. Torquato, Phys. Rev. Lett. **74**, 2156 (1995); Phys. Rev. E **51**, 3170 (1995).  
 [8] J. Rubinstein and S. Torquato, J. Fluid Mech. **206**, 25 (1989).  
 [9] S. Torquato and J. Rubinstein, J. Chem. Phys. **90**, 1644 (1989).  
 [10] J. G. McNally and E. C. Cox, Development **105**, 323 (1989).  
 [11] P. Hertz, Math. Ann. **67**, 387 (1909).  
 [12] M. D. Rintoul, S. Torquato, and G. Tarjus, Phys. Rev. E **53**, 450 (1996).  
 [13] P. Viot, G. Tarjus, and J. Talbot, Phys. Rev. E **48**, 480 (1993).  
 [14] P. Wojtaszczyk, P. Schaaf, B. Senger, M. Zembala, and J. C. Voegel, J. Chem. Phys. **99**, 7198 (1993).  
 [15] J. Talbot and S. Ricci, Phys. Rev. Lett. **68**, 958 (1992).  
 [16] D. Boyer, G. Tarjus, and P. Viot, J. Phys. A **29**, 2309 (1996).  
 [17] A. Rényi, Sel. Trans. Math. Stat. Prob. **4**, 205 (1963).  
 [18] R. J. Baxter, J. Chem. Phys. **49**, 2770 (1968).